REPORT SSD-TR-89-77

4

Spectroscopic Techniques for the Analysis of CdTe Substrates Used for the Growth of HgCdTe

Prepared by

D. E. COOPER and J. BAJAJ
Rockwell International Science Center
Thousand Oaks, CA 91360

and

R. C. BOWMAN, JR.
Chemistry and Physics Laboratory
Laboratory Operations
The Aerospace Corporation
El Segundo, CA 90245

25 September 1989

Prepared for

SPACE SYSTEMS DIVISION
AIR FORCE SYSTEMS COMMAND
Los Angeles Air Force Base
P.O. Box 92960
Los Angeles, CA 90009-2960

This report was submitted by The Aerospace Corporation, El Segundo, CA 90245, under Contract No. F04701-88-C-0089 with the Space Systems Division, P.O. Box 92960, Los Angeles, CA 90009-2960. It was reviewed and approved for The Aerospace Corporation by S. Feuerstein, Director, Chemistry and Physics Laboratory. Capt David Sanders was the project officer for the Mission-Oriented Investigation and Experimentation (MOIE) Program.

This report has been reviewed by the Public Affairs Office (PAS) and is releasable to the National Technical Information Service (NTIS). At NTIS, it will be available to the general public, including foreign nationals.

This technical report has been reviewed and is approved for publication. Publication of this report does not constitute Air Force approval of the report's findings or conclusions. It is published only for the exchange and stimulation of ideas.

DAVID SANDERS, CAPT, USAF
MOIE Project Officer
SSD/CNSE

RAYMOND M. LEONG, MAJ, USAF
MOIE Program Manager
AFSTC/WCO OL-AB

REPORT DOCUMENTATION PAGE

1a. REPORT SECURITY CLASSIFICATION Unclassified	1b. RESTRICTIVE MARKINGS
2a. SECURITY CLASSIFICATION AUTHORITY -	3. DISTRIBUTION/AVAILABILITY OF REPORT Approved for public release; distribution unlimited.
2b. DECLASSIFICATION/DOWNGRADING SCHEDULE	
4. PERFORMING ORGANIZATION REPORT NUMBER(S) TR-0089(4945-07)-3	5. MONITORING ORGANIZATION REPORT NUMBER(S) SSD-TR-89-77
6a. NAME OF PERFORMING ORGANIZATION The Aerospace Corporation Laboratory Operations 6b. OFFICE SYMBOL (If applicable)	7a. NAME OF MONITORING ORGANIZATION Space Systems Division
6c. ADDRESS (City, State, and ZIP Code) El Segundo, CA 90245-4691	7b. ADDRESS (City, State, and ZIP Code) Los Angeles Air Force Base Los Angeles, CA 90009-2960
8a. NAME OF FUNDING/SPONSORING ORGANIZATION 8b. OFFICE SYMBOL (If applicable)	9. PROCUREMENT INSTRUMENT IDENTIFICATION NUMBER F04701-88-C-0089
8c. ADDRESS (City, State, and ZIP Code)	10. SOURCE OF FUNDING NUMBERS PROGRAM ELEMENT NO. / PROJECT NO. / TASK NO. / WORK UNIT ACCESSION NO.

11. TITLE (Include Security Classification)

Spectroscopic Techniques for the Analysis of CdTe Substrates Used for the Growth of HgCdTe

12. PERSONAL AUTHOR(S) Cooper, D. E., Bajaj, J. (Rockwell International Science Center) and Bowman, R. C. Jr. (The Aerospace Corporation)

13a. TYPE OF REPORT	13b. TIME COVERED FROM ____ TO ____	14. DATE OF REPORT (Year, Month, Day)	15. PAGE COUNT
		1989 September 25	25

16. SUPPLEMENTARY NOTATION-

17. COSATI CODES			18. SUBJECT TERMS (Continue on reverse if necessary and identify by block number)
FIELD	GROUP	SUB-GROUP	Photoluminescence; Spectrometer; Photoluminescence signature; Cathodoluminescence

19. ABSTRACT (Continue on reverse if necessary and identify by block number)

Photoluminescence (PL) and electron paramagnetic resonance (EPR) are powerful techniques for both fundamental studies and potential materials screening of CdTe substrates for HgCdTe growth. Certain extended defects that are common in epitaxial CdTe have distinctive PL signature that correlates with X-ray measurements of crystallinity. Bulk samples with prominent subgrain structure also have this PL feature, and cathodoluminescence images show that the defect is localized to the subgrain boundary regions. PL and EPR are very sensitive techniques, and specific impurities such as Fe or Ag have been observed in some nominally pure samples. PL and EPR spectroscopy can also detect changes associated with thermal annealing treatments, which alter the stoichiometry of CdTe by varying the number of Cd vacancies and interstitials. These findings illustrate the versatility of PL and EPR as nondestructive techniques to assess the quality of substrates for IR-detector materials.

-

20 DISTRIBUTION/AVAILABILITY OF ABSTRACT	21. ABSTRACT SECURITY CLASSIFICATION
☒ UNCLASSIFIED/UNLIMITED ☐ SAME AS RPT. ☐ DTIC USERS	Unclassified
22a. NAME OF RESPONSIBLE INDIVIDUAL	22b. TELEPHONE (Include Area Code) / 22c. OFFICE SYMBOL

PREFACE

We wish to thank P. Smith of Caltech for his assistance with the EPR measurements used in this report. The work at The Aerospace Corporation was supported by the U.S. Air Force Space Systems Division under Contract No. F04701-85-C-0086.

CONTENTS

FIGURES

I. INTRODUCTION

CdTe is often used as a substrate for the epitaxial growth of HgCdTe (MCT), and the crystallinity and purity of the CdTe substrate directly affects the quality of the MCT epilayers. Crystalline defects in the substrate can extend into the epilayer, so selection of substrates with a minimum of dislocations and other extended defects is desirable. Impurities present in the substrate can also diffuse into the epilayers during high-temperature growth, leading to unintentional doping. We have used a variety of spectroscopic tools, including photoluminescence (PL), cathodoluminescence (CL), and electron paramagnetic resonance (EPR) to develop screening techniques for CdTe substrates. In this report we will show how these techniques can be used to determine the crystallinity of CdTe and to detect and identify specific impurities at very low concentrations.

Photoluminescence has been used for many years to study CdTe, and a considerable body of literature has been produced.[1-3] Even very small impurity concentrations (parts-per-billion level) produce PL features that dominate the spectrum. In relatively pure crystalline samples, the PL spectra are dominated by very narrow (1.0 meV) bound exciton lines near the band-edge energy. At lower photon energies, relatively broad donor-acceptor pair (DAP) bands are produced by the recombination of carriers on donor and acceptor impurities. In many cases specific impurities have been associated with certain PL lines, making it possible to detect impurities at very low concentrations.[3] In samples with poor crystallinity, distinctive PL bands have been associated with extended defects.[4] Because of the diverse information that it provides, photoluminescence has become a standard technique for evaluating material produced by advanced growth methods such as MOCVD and MBE.

Various impurities (e.g., transition metals and donors), point defects (e.g., vacancies and interstitials), and defect complexes (e.g., vacancy-

donor associates) in elemental and compound semiconductors can be detected and often identified via their electron paramagnetic resonance spectra.[5,6] Although defect concentrations as low as 10^{15} cm^{-3} may be studied in bulk II-VI and elemental semiconductors,[6] these centers must be in a paramagnetic state and must satisfy numerous experimental critieria (i.e., linewidths less than a few gauss, intermediate spin-lattice relaxation times, low electrical conductivity, etc.). However, simultaneous illumination with light during the EPR measurements (i.e., photo-EPR) can sometimes convert diamagnetic defects into paramagnetic centers that are amenable to EPR analysis as well as alter the characteristics and populations of existing paramagnetic species. Through the hyperfine interactions with the nuclear moments of impurities and host lattice atoms, unequivocal assignments of the composition and microscopic structure of these defects can be made.[6]

II. EXPERIMENTAL

Samples for PL spectroscopy were etched in Br/CH_3OH solution prior to mounting in a liquid helium dewar. Samples were cooled to 2 K for high resolution spectra and to 4.2 K for low resolution spectra. The optical excitation source was a 0.5 mW HeNe laser focussed to about 1 W/cm^2 with a cylindrical lens. To obtain low resolution (0.3 nm) spectra, the PL was dispersed in a 1/4 m spectrometer and detected with a 1024-element intensified diode array. High resolution (0.02-0.04 nm) spectra were obtained by dispersing the PL in a 3/4 m double spectrometer and detecting the radiation with a photomultiplier tube (PMT) and phase-sensitive detection electronics.

Cathodoluminescence (CL) experiments were performed in the laboratory of Prof. Petroff at the University of California at Santa Barbara. Samples were cooled to 8 K. CL was excited by a 150 keV electron beam, dispersed by a spectrometer, and detected with a PMT. This equipment could be operated by fixing the detection wavelength and rastering the electron beam to create images, or by fixing the electron beam position on a feature and scanning the detection wavelength to create a CL spectrum.

The EPR experiments used a Varian E-line spectrometer at the California Institute of Technology. One wall of the X-band microwave cavity was slotted to permit illumination with unfiltered light from 200 W Hg-Xe or Xe lamps while the samples were cooled to temperatures between 5 K and 20 K. While no significant effects could be attributed to the temperature variations, the presence or absence of light did change the EPR signals for many of the investigated CdTe samples.

III. PHOTOLUMINESCENCE FROM EXTENDED DEFECTS

Photoluminescence can be used to evaluate the crystallinity of semiconductors when specific PL bands can be identified with extended defects. In CdTe a PL band peaking at 842 nm has been associated with a crystalline defect in epitaxial layers.[4,7] Epitaxial CdTe is often used as a buffer layer between HgCdTe and a substrate with a different lattice parameter, so it is important to minimize the misfit dislocations in these layers. The distribution of intensity among the LO phonon replicas in this band shows weak phonon coupling, which suggests that this band is related to an extended defect.[4] This band is distinct from the defect band originating at 850 nm in low-quality bulk CdTe samples,[8] which has a spectrum indicating a greater phonon coupling. The PL intensity of the 842 nm band varies with growth conditions. Figure 1 shows three low-resolution PL spectra obtained from MBE CdTe samples grown on CdTe at three different substrate temperatures. In each spectrum the dominant emission is from donor-acceptor pair (DAP) recombination associated with shallow donors and acceptors. The defect peak at 842 nm shows substantial variation in amplitude, with the largest peak seen in the epilayers grown at the lowest substrate temperature. At 220°C the mobility of the Cd and Te atoms on the surface of the crystal is not great enough to grow a well-ordered crystal lattice, leading to the formation of extended defects. This trend is also reflected in the width of the X-ray rocking curve ($\Delta\theta$), which correlates with the defect emission amplitude. This direct correlation with a standard diagnostic of material crystallinity confirms that the 842 nm peak is due to extended defects.

Although the 842 nm defect peak is very common in the PL spectra of low-quality MBE and MOCVD CdTe films, we believe we are the first to report this peak in the spectra of bulk CdTe crystals. Figure 2 shows a CL spectrum of a bulk CdTe sample, which indicates a prominent peak at 842 nm. CL makes it possible to produce spatial maps of the emission at particular wavelengths, and Fig. 3 shows two such images using wavelengths

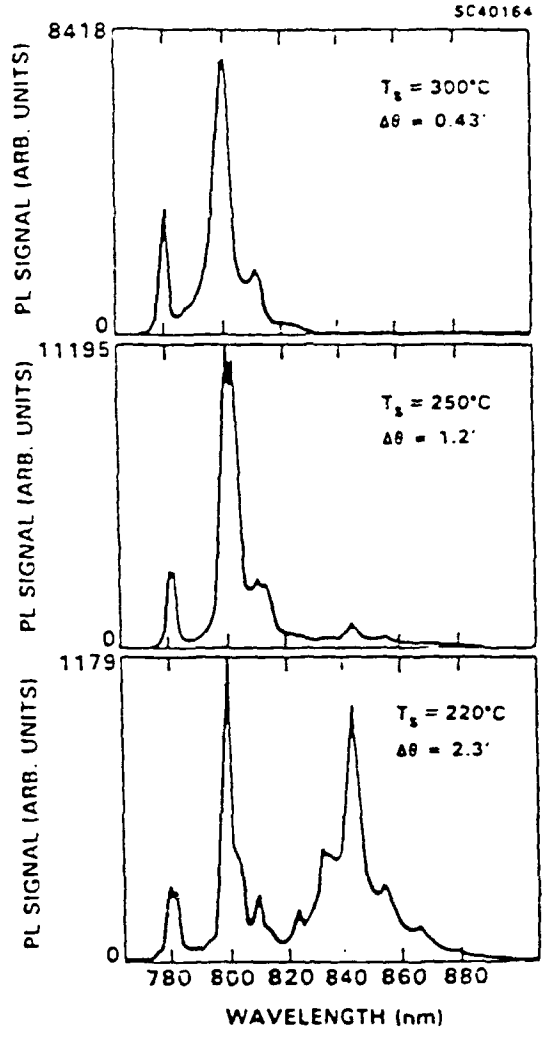

Fig. 1. PL Spectra of Three MBE-Grown CdTe Samples with Varying Substrate Temperatures. Both the X-ray rocking curve width width ($\Delta\theta$) and the amplitude of defect emission at 842 nm vary with the substrate temperatures.

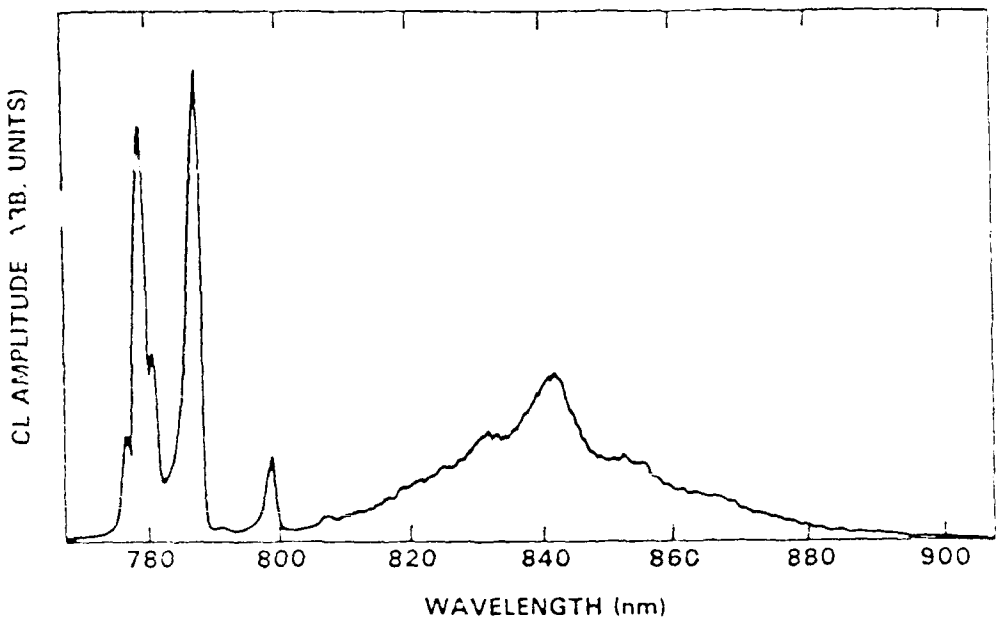

Fig. 2. CL Spectrum of Bulk CdTe Sample Showing Characteristic Defect Peak at 842 nm. The excitation was localized to a grain boundary.

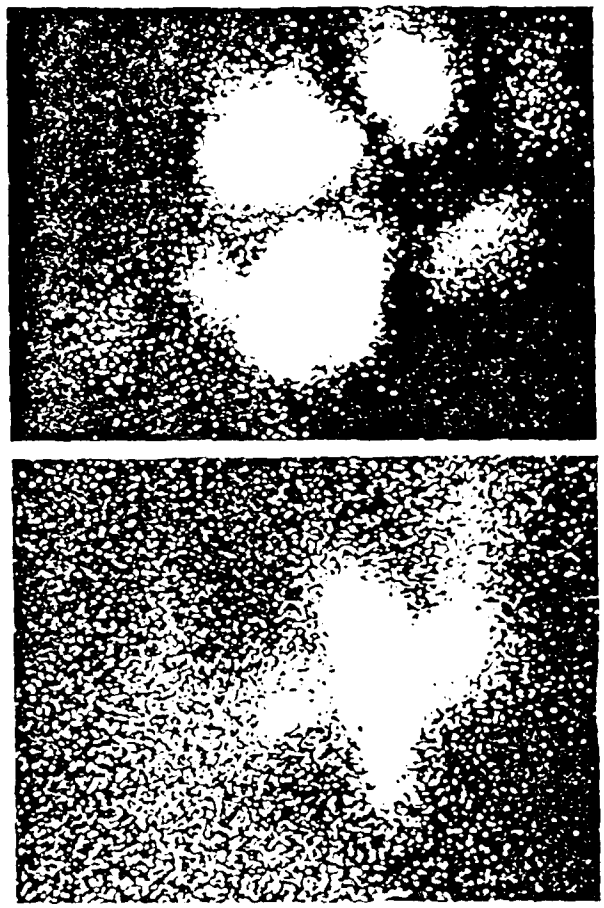

Fig. 3. CL Images of Band Edge Emission (top) and Defect Emission (bottom) in Bulk CdTe. The defect emission is localized in the grain boundary regions.

near the band edge (785 nm) and near the defect peak (851 nm). These images show that the band-edge emission comes from crystalline subgrains and the defect emission comes from the subgrain boundaries. (The spectrum shown in Fig. 2 was obtained by exciting a subgrain boundary.) These data show that the 842 nm defect emission is also present in bulk CdTe samples, but only from the low-quality subgrain boundary regions. Defects from the subgrain boundaries are believed to propagate into epilayers grown on these CdTe samples, and much effort has gone into growing CdTe wafers with minimal subgrain structure. PL and CL spectroscopy can be important tools in detecting the presence of this particular defect.

IV. DETECTION AND IDENTIFICATION OF IMPURITIES

The electrical properties of semiconductors can be dominated by trace amounts of impurities, and the detection and identification of unintentional dopants is vital to the production of improved semiconductor devices. PL and and EPR spectra often provide distinctive "fingerprints" that can be used to identify specific impurities. In this section we will discuss the use of PL and EPR to identify the presence of iron and silver impurities in CdTe.

Iron forms a deep donor in CdTe, and iron-implanted CdTe wafers display a very distinctive EPR signal and a PL band at about 1.1 micron.[9] Iron impurities in MCT have been associated with a reduction in the minority carrier lifetime,[10] and therefore the elimination of iron in CdTe substrates for MCT growth is particularly important. Detecting iron impurities in CdTe by mass spectrometric techniques is difficult since the atomic mass of iron is half that of cadmium.

We have used PL and EPR to survey about two dozen CdTe samples from a variety of sources, and have found that many of them contain iron at easily detectable levels.[11] Figure 4 shows the Fe^{+3} EPR signal for a nominally pure sample that contains substantial quantities of iron. The complex iron signal is highly anisotropic, but it is easily distinguished from common shallow donors, which produce a single peak at about 3900 G ($g = 1.694$). The Pl spectrum of this sample is given in Fig. 5a, and it shows a large peak at 1.1 microns. In contrast, the Pl spectrum of a sample that has no Fe^{+3} EPR signal (Fig. 5b) has a very weak peak at 1.1 microns. (The weak 1.1 micron peak seen in Fig. 5b is probably due to deep levels associated with other impurities or defects.) The amplitudes of the PL and EPR signals due to iron in the samples we examined were found to be correlated, suggesting that both techniques give a potentially quantitative measure of iron contamination. In an effort to relate the amplitudes of these signals to independent quantitative measurements of iron contents, two samples were

analyzed by secondary ion mass spectrometry (SIMS). Although one sample showed large PL and EPR iron signals and the other showed negligible iron signals, both samples had SIMS signals corresponding to 0.1 ppm iron concentration, indicating that this is the background level due to Cd^{+2} interference. We are currently working to obtain samples with measurable iron concentrations so that the spectroscopic techniques can be calibrated. Clearly both the PL and EPR techniques are able to detect iron contamination of CdTe at levels < 0.1 ppm. This sensitivity is surpassed only by destructive techniques using large (> 1 g) samples.

The surface quality of substrates is crucial for high-quality MBE and MOCVD growth, and noncontact hydro-polishing is used to minimize surface defects. Hydro-polished samples have PL spectra that are generally similar to deeply etched samples, which indicates that hydro-polishing does not create a layer of surface defects. Although the PL spectra of the hydro-polished substrates do not show any surface damage, they give evidence of surface contamination by silver.

Surface contamination by silver was seen in all three CdTe samples chosen for this study:

Sample No. 1: Grown, cut, and polished by the II-VI Corp.

Sample No. 2: Grown at II-VI, cut, and polished at Rockwell.

Sample No. 3: Grown, cut, and polished at Rockwell.

Each sample was cleaved into two pieces, and one piece received a light clean-up etch (10 seconds in 1/2% Br/CH_3OH, removing about 0.25 microns) and the other was heavily etched (2 minutes in 2% Br/CH_3OH, removing about 10 microns). In each case, the PL intensity was approximately equal for the two pieces, indicating that the surface was relatively free of PL-quenching defects. However, each pair of samples showed a difference in the high-resolution spectra of the narrow peaks due to recombination of excitons bound to neutral acceptors. Figure 6 shows the dramatic difference in the spectra produced by Sample No. 2. These bound exciton lines have been assigned to specific impurities,[3] and the peak at 780.3 nm

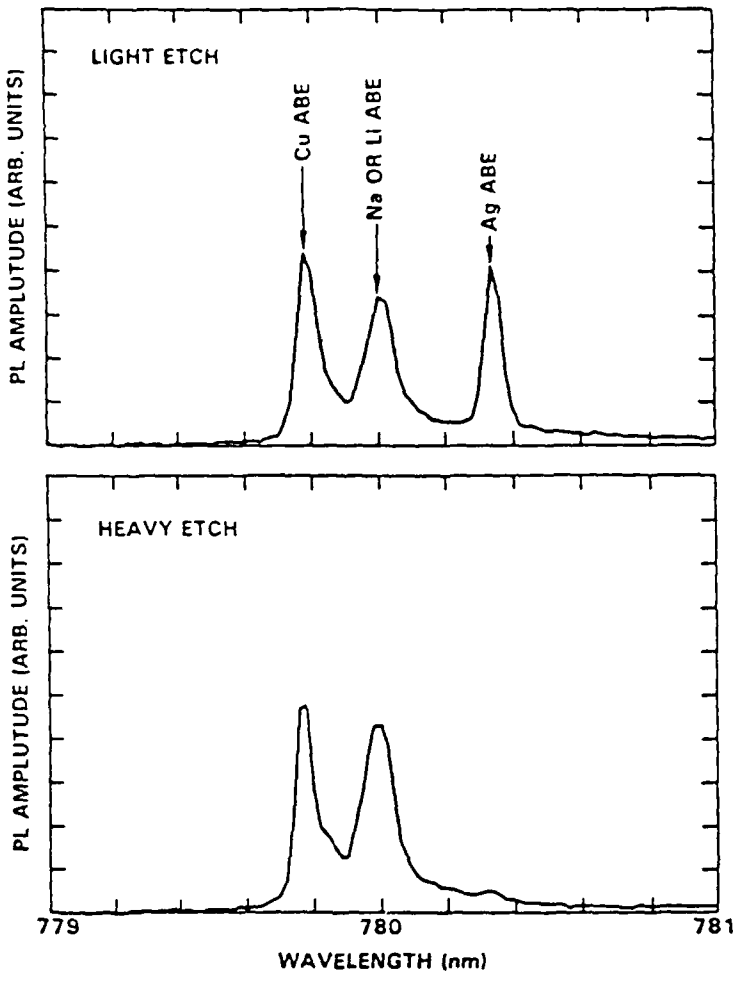

Fig. 6. High Resolution PL Spectra of CdTe Acceptor-Bound Exciton (ABE) Peaks. Top spectrum is from lightly etched sample, bottom is heavily etched sample from same wafer.

has been attributed to silver impurities. In each pair of samples two of the bound exciton lines did not vary with sample etch, but the line due to Ag impurities was reduced by a factor of 5-23 by the deep etch. This indicates that the Ag contamination is confined to the first few microns, and is very likely due to the polishing process.

The amplitude of the bound exciton emission from the Ag peak in Fig. 6 is equal to that of the other two acceptor-bound excitons. This is due primarily to the lower energy of this bound exciton, and does not indicate

that the Ag concentration is equal to that of the other two acceptors. This was confirmed by PL spectra at higher sample temperatures, which showed relatively low Ag-bound exciton emission. Thus, the Ag acceptor concentration is considerably lower that of the other acceptors. However, Ag forms a relatively deep acceptor level,[3] which could lead to enhanced Shockley-Read-Hall recombination and reduced carrier lifetime if the Ag diffused into MCT epilayers grown on the CdTe.

V. STOICHIOMETRIC DEVIATIONS

Cadmium telluride crystals grown from the melt are typically slightly deficient in Cd, leading to the formation of Te precipitates and Cd vacancies. We have studied changes in the PL and EPR spectra due to variations in crystal stoichiometry caused by annealing CdTe wafers in a Cd atmosphere. Wafers were sealed in evacuated quartz tubes with elemental Cd and were heated for 2-3 days at 500-600°C. After annealing, about 20 microns were etched from the surface. The changes produced by this annealing procedure are complex and include changes in the electrically active impurities as well as stoichiometric variations. The PL and EPR spectra change significantly after Cd annealing, and thus give valuable insight into the Cd annealing process by determining changes in the donor and acceptor concentrations and by identifying specific acceptor species.

The principal changes expected from Cd annealing are a reduction in the concentration of Cd vacancies and the possible formation of Cd interstitials. Since the Cd vacancy is a double acceptor and the Cd interstitial is a double donor, the as-grown p-type CdTe material will tend to become n-type upon annealing. This is reflected in the relative amplitudes of the PL lines due to excitons bound on neutral donors and acceptors. Figure 7 shows low-resolution PL spectra of a sample before and after Cd annealing. The spectrum of the p-type as-grown sample shows a negligible DBE peak, but after annealing the DBE peak is much larger than the ABE peak. The increase in the donor concentration could be due to formation of Cd interstitials, but it could also be caused by the release of donor impurities dissolved in Te precipitates, which are reduced by the anneal.[3]

Another major difference in the spectra in Fig. 7 is the elimination of the peak at 804 nm after Cd annealing. This peak is due to donor-acceptor pair (DAP) recombination involving shallow donors and acceptors, and the change indicates that the concentration of shallow acceptors has

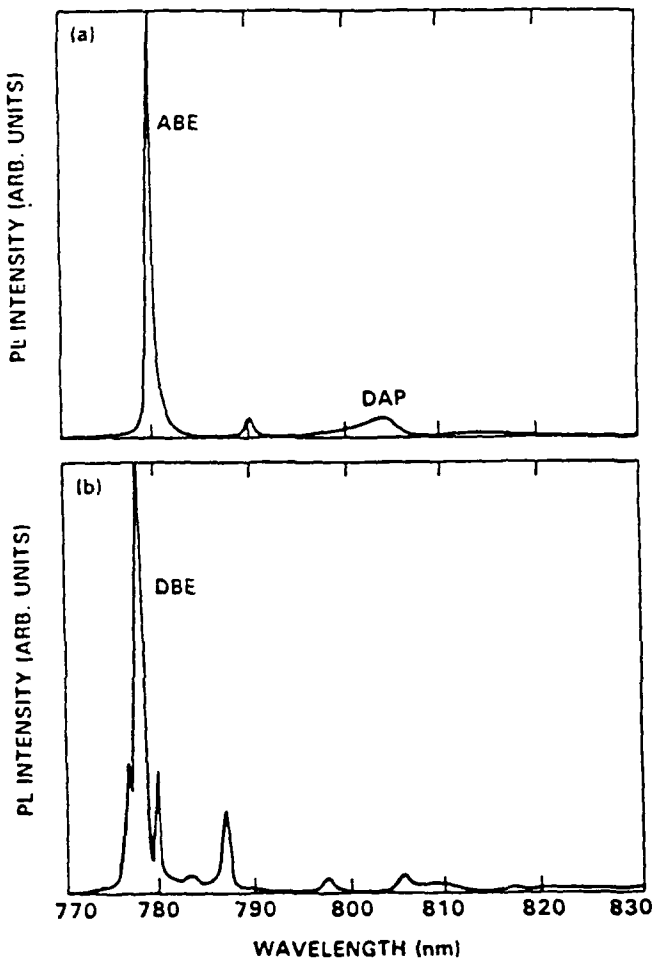

Fig. 7. PL Spectra of CdTe Samples Before (Top) and After (Bottom) Cd Annealing

been reduced by Cd annealing. The acceptors involved in this process are throught to be Group I elements (such as Na and Li) on Cd sites. SIMS studies have also seen a reduction in these species after Cd annealing,[12] and it is likely that they are displaced by Cd and migrate to the sample surface.

The reduction in Group I acceptors is accompanied by an activation of Group V acceptors, which occupy a Te site. The weak PL band at 810 nm is due to DAP recombination involving P, and the peak at 805 nm is caused by the recombination of free electrons and neutral phosphorous acceptors.[13] Activation of Group V acceptors is difficult,[14] probably because of their ability to occupy the Cd site in Cd-deficient material and compensation by Cd interstitials in Cd-rich materials.

The change in acceptor species upon Cd annealing can be understood in terms of a simple mass action effect. As the sample changes from Cd-deficient to Te-deficient, the active acceptors change from those that occupy Cd sites (Group I) to those that occupy Te sites (Group V). Since the Group I acceptors are relatively common impurities such as Na and Li, the net effect of Cd annealing is to purify the CdTe material. The Group I elements also rapidly diffuse through CdTe, and therefore they are more likely to cause contamination of HgCdTe epilayers grown on CdTe substrates. For these reasons Cd annealing can be a beneficial treatment for CdTe substrates. In Fig. 7 the improvement in the purity of the sample is reflected in the relatively large free exciton emission (at 777 and 787 nm) for the Cd-annealed samples.

The Cd annealing treatments also produced changes in the EPR spectra for many of the CdTe crystals. In those samples (e.g., No. 2438 or 4-11) where Fe^{+3} signals were present[11] when unannealed, these distinctive EPR peaks disappeared after the 600°C anneals under the Cd-vapor overpressure. This behavior can be attributed to the Fermi level moving above the Fe^{+3}/Fe^{+2} transition state in the band gap as the Cd vacancies are eliminated. Although Fe^{+2} could conceivably give an EPR spectrum,[15] there was no indication for a paramagnetic Fe^{+2} center in any of these studies. However, the anneals sometimes gave a new isotropic EPR peak with $g = 1.69$ (see Table 1). According to Saminadayar, et al.,[16] this peak corresponds to shallow donors from impurities such as Cl [$g = 1.684(1)$], In[$g = 1.704(1)$], or Al [$g = 1.65(1)$]. Figure 8 presents our EPR results from a high-resistivity CdTe crystal (No. 4011) doped with In at a nominal

Table 1. EPR Parameters for Shallow Donor Impurities in CdTe Crystals

Sample Number	Cd-Vapor Annealed @ 600°C	Xe Lamp Illuminated	G-Factor	ΔHpp (gauss)	Comments
4011	No	Yes	1.693(1)	16(3)	In doped @ 2×10^{17} cm^{-3} (no signal in dark)
2-42	No	No	1.6925(20) 1.6931(30)	11(2) 6(2)	
2-42	Yes	No Yes	1.6913 1.6912	6.1 3.8	
2-48	No	Yes	1.6993	10	No signal in dark
2-51	No	Yes	1.70	-	Very weak peak
4-7	No	No Yes	1.6934 1.6925	20 20	Fe^{+3} peaks seen
4-10	No	No	ND*	-	Fe^{+3} peaks seen
4-10	Yes	No	1.693	22	Could not tune with lamp on
4-11	No	No/Yes	ND*	-	Fe^{+3} peaks seen
4-11	Yes	No	1.691	-	Two overlapping peaks (nothing when unannealed
		Yes	1.693	4.0	Single peak
QZR-217	Yes	No Yes	1.687 1.687	10 10	Very weak (nothing when unannealed)

*No signal detected.

concentration of 2×10^{17} cm^{-3}. No signal is observed when the crystal is in the dark, but a peak at $g = 1.693$ is present during irradiation with a focused, unfiltered lamp. The electrons created by illumination presumably neutralize the originally compensated In donors in these unannealed crystals. When the light from the lamp is blocked, the donor EPR rapidly vanishes but reappears when the sample is illuminated again. Although some nominally undoped CdTe crystals also gave the donor EPR peak without annealing (apparently from accidential impurities), the Cd-anneals either enhanced its intensity or generated it in most cases. The properties of the EPR signals associated with shallow donors in several CdTe samples are summarized in Table 1. In nearly every case the g-factors are indistinguishable (within experimental accuracy) from the value obtained from the In-doped crystal. However, it is not necessarily the primary donor impurity even though Saminadayar, et al.[16] did report different g-factors for various dopants. Unfortunately, simply too many uncontrolled factors can influence the EPR parameters to permit a reliable assignment. For example, the peak-to-peak linewidths (ΔHpp) vary among the samples and also change with illumination as shown in Fig. 9. At least one annealed sample (No. 4-11, Fig. 9b) gave two partially resolved peaks in the dark but a single, sharp peak when illuminated. The asymmetric line-shapes for some other annealed samples may be due to less well resolved peaks from different donors. The narrowing of the donor peaks during illumination (Fig. 9a) is consistent with enhanced spin-exchange interactions[16] from increased concentration of neutral donors. Additional studies are under way to determine whether the small differences in g-factors can be due to different donor impurities and correlated with the donor-like peaks in the PL spectra.

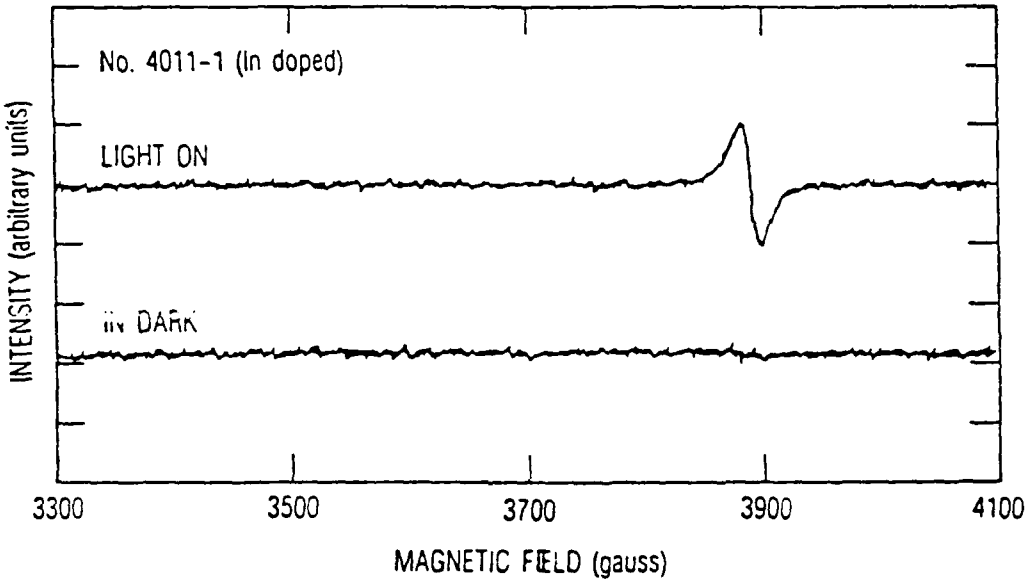

Fig. 8. EPR Spectra from an In-Doped CdTe Crystal (No. 4011)

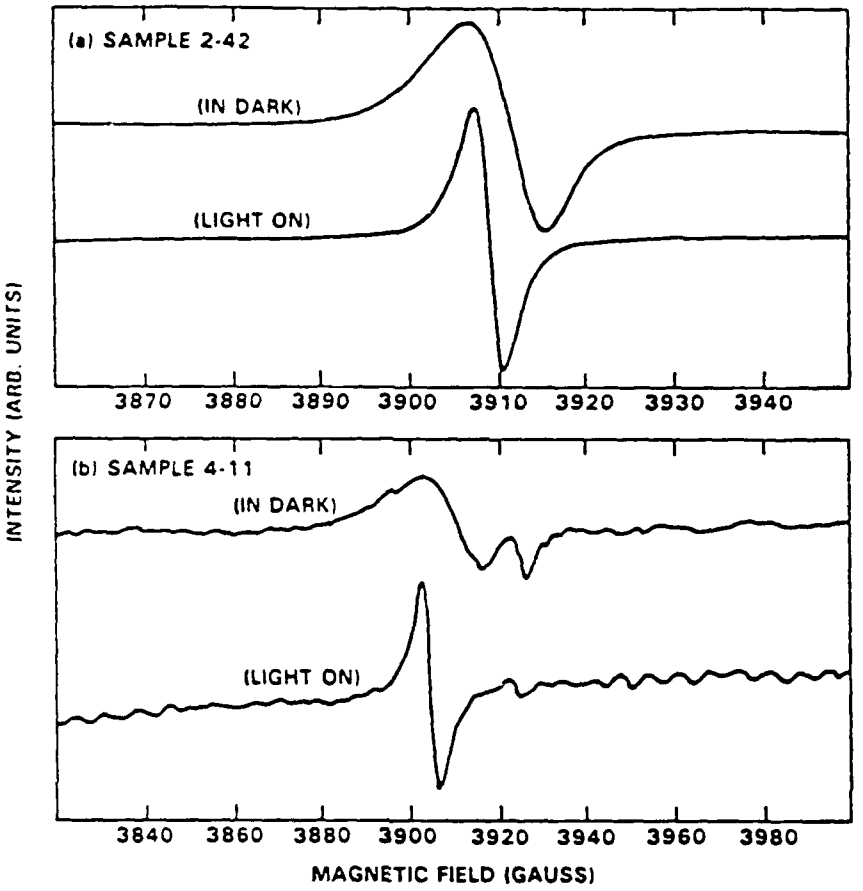

Fig. 9. EPR Spectra of Donor Centers in CeTe Crystals That Were Annealed at 600°C in Cd Vapor, Showing the Changes Produced by Illumination

6. SUMMARY

In this report we have surveyed various spectroscopic techniques for the evaluation of CdTe for use as substrates for the growth of HgCdTe. Although PL, CL, and EPR do not usually give the quantitative information obtained from mass spectrometric analysis (such as SIMS), for relatively pure material they can be more sensitive, especially in cases where there is interference from the dominant atomic species. In epitaxial material, which often has a high defect density, these techniques also provide information about the crystallographic quality of the material, which is vital for the use of CdTe as an epitaxial substrate. This diversity of information makes PL, CL, and EPR very useful diagnostic techniques for CdTe substrates.

REFERENCES

1. P. Hiesinger, S. Suga, F. Willimann, and W. Dreybrodt, Phys. Stat. Sol. B67, 641 (1975).

2. A. Nakamura and C. Weisbuch, Solid State Elect. 21, 1331 (1978).

3. J. L. Pautrat, J. M. Francou, N. Magnea, E. Molva, and K. Saminadayar, J. Crystal Growth 72, 194 (1985).

4. P. J. Dean, G. M. Williams, and G. Blackmore, J. Phys. D17, 2291 (1984).

5. R. S. Title, in Physics and Chemistry of II-VI Compounds, edited by M. Aven and J. S. Prener (American Elsewhere, New York, 1967) p. 265.

6. J. Scheinder, Mat. Res. Soc. Symp. Proc. 46, 13 (1985).

7. Z. C. Feng, A. Mascarenhas, and W. J. Choyke, J. Lumin. 35, 329 (1986).

8. C. B. Norris and C. E. Barnes, Rev. Phys. Appl. 12, 219 (1977).

9. R. Kernocker, K. Lischka and L. Palmetshofer, J. Crystal Growth 86, 675 (1988).

10. P. Capper, J. Crystal Growth 57, 280 (1982).

11. R. C. Bowman, Jr. and D. E. Cooper, Appl. Phys. Lett. 53, 1521 (1988).

12. L. L. Bubulac, W. E. Tennant, D. D. Edwall, E. R. Gertner, and J. C. Robinson, J. Vac. Sci. Technol. A3, 163 (1985).

13. E. Molva, K. Saminadayer, J. L. Pautrat, and E. Ligeon, Sol. St. Commun. 48, 955 (1983).

14. M. Chu, R. H. Bube, and J. F. Gibbons, J. Electrochem. Soc. 127, 483 (1980).

15. A. Abragam and B. Bleaney, Electron Paramagnetic Resonance of Transition Ions (Dover, New York, 1986), Chapter 7.

16. K. Saminadayar, D. Galland, and E. Molva, Solid State Commun. 49, 627 (1984).

LABORATORY OPERATIONS

The Aerospace Corporation functions as an "architect-engineer" for national security projects, specializing in advanced military space systems. Providing research support, the corporation's Laboratory Operations conducts experimental and theoretical investigations that focus on the application of scientific and technical advances to such systems. Vital to the success of these investigations is the technical staff's wide-ranging expertise and its ability to stay current with new developments. This expertise is enhanced by a research program aimed at dealing with the many problems associated with rapidly evolving space systems. Contributing their capabilities to the research effort are these individual laboratories:

Aerophysics Laboratory: Launch vehicle and reentry fluid mechanics, heat transfer and flight dynamics; chemical and electric propulsion, propellant chemistry, chemical dynamics, environmental chemistry, trace detection; spacecraft structural mechanics, contamination, thermal and structural control; high temperature thermomechanics, gas kinetics and radiation; cw and pulsed chemical and excimer laser development including chemical kinetics, spectroscopy, optical resonators, beam control, atmospheric propagation, laser effects and countermeasures.

Chemistry and Physics Laboratory: Atmospheric chemical reactions, atmospheric optics, light scattering, state-specific chemical reactions and radiative signatures of missile plumes, sensor out-of-field-of-view rejection, applied laser spectroscopy, laser chemistry, laser optoelectronics, solar cell physics, battery electrochemistry, space vacuum and radiation effects on materials, lubrication and surface phenomena, thermionic emission, photosensitive materials and detectors, atomic frequency standards, and environmental chemistry.

Computer Science Laboratory: Program verification, program translation, performance-sensitive system design, distributed architectures for spaceborne computers, fault-tolerant computer systems, artificial intelligence, microelectronics applications, communication protocols, and computer security.

Electronics Research Laboratory: Microelectronics, solid-state device physics, compound semiconductors, radiation hardening; electro-optics, quantum electronics, solid-state lasers, optical propagation and communications; microwave semiconductor devices, microwave/millimeter wave measurements, diagnostics and radiometry, microwave/millimeter wave thermionic devices, atomic time and frequency standards; antennas, rf systems, electromagnetic propagation phenomena, space communication systems.

Materials Sciences Laboratory: Development of new materials: metals, alloys, ceramics, polymers and their composites, and new forms of carbon; nondestructive evaluation, component failure analysis and reliability; fracture mechanics and stress corrosion; analysis and evaluation of materials at cryogenic and elevated temperatures as well as in space and enemy-induced environments.

Space Sciences Laboratory: Magnetospheric, auroral and cosmic ray physics, wave-particle interactions, magnetospheric plasma waves; atmospheric and ionospheric physics, density and composition of the upper atmosphere, remote sensing using atmospheric radiation; solar physics, infrared astronomy, infrared signature analysis; effects of solar activity, magnetic storms and nuclear explosions on the earth's atmosphere, ionosphere and magnetosphere; effects of electromagnetic and particulate radiations on space systems, space instrumentation.

...